RNI Regd No: APENG/2011/47294 ISSN No: 2320-3706(PRINT)
International Journal & Magazine of Engineering, Technology, Management and Research
YUVAENGINEERS
Transforming Young Engineers for Better Tomorrow

Modeling and Design of Series Voltage Compensator for Reduction of DC-Link Capacitance in Grid-Tie Solar Inverter

Boosharaju Ravi Kumar
Research Scholar,
Department of Power Systems,
SRTIST Engineering College,
Nalgonda, India.

Dr.Y.R.Manjunath
Professor,
Department of Power Systems,
SRTIST Engineering College,
Nalgonda, India.

ABSTRACT:

A grid-tie solar inverter with a series voltage compensator for reducing the high-voltage dc-link capacitance is presented. The compensator obtains energy fromthe dc link to sustain the voltage on its dc side and generates an ac voltage to counteract the voltage ripple on the dc link. As the compensator processes small ripple voltage on the dc link and reactive power, it can be implemented with low-voltage devices, and thus, its voltamp rating is small. As the required energy storage of the dc link, formed by a reduced value of the dc-link capacitor and the compensator, is reduced, the architecture allows replacing popularly used electrolytic capacitors with alternatives of longer lifetime, such as power film capacitors, or extending the system lifetime even if there is a significant reduction in the capacitance of electrolytic capacitors due to aging. Detailed mathematical analysis on the static and dynamic behaviors of the overall system, and the control method will be presented. A simplified design procedure for the compensator will be given. A 2-kW, 220-V, 50-Hz prototype has been built and evaluated. The theoretical predictions are compared favorably with experimental results. Finally, the implementation cost with electrolytic-capacitor and compensator for the dc link will be compared.

INTRODUCTION:

In today's eco-conscious world, the rapid pace of advancement in smart grid technology has a positive effect on the electricity industry reforms. The goal is to use smarter control of distributed energy sources combined with intelligent demand side management to improve the overall efficiency and reliability of the power grid. Regardless of the type of the distributed power generation unit used, the electricity generated by the renewable energy source is processed through a power conditioning system that performs several functions. First, it fabricates an optimal power matching condition for the renewable energy source to deliver maximum power to the power conditioning system. Second, it manages energy flow among the renewable energy source, energy storage system, and surrounding ac and/or dc networks or systems. Third, it produces high-quality power to and from the energy storage system, loads, and connected grid. Finally, it is capable of providing tight output regulation and handling fast transient and dynamic response to external disturbances. Typical power conditioning systems consist of multiple switching-mode power converters.

In order to provide high degree of controllability and flexibility of power flow, the electrical energy generated by renewable energy source is converted into dc power while the one delivered to the other part of the system or load is converted from the dc power. Thus, power converters are all interconnected through a dc link. To ensure a stable operation of the power conditioning system, the dc-link voltage is stabilized by a capacitor bank, which is sometimes the dominant part in terms of the physical volume and cost. Among the different types of capacitors, aluminum electrolytic capacitors are a popular choice for the capacitor bank, due to their high capacitances in a small form factor. However, their life expectancy is comparatively short and is reduced dramatically with elevated ambient temperatures.

RNI Regd No: APENG/2011/47294 ISSN No: 2320-3706(PRINT)
International Journal & Magazine of Engineering, Technology, Management and Research
YUVAENGINEERS
Transforming Young Engineers for Better Tomorrow

Statistics reveals that up to 30% of electronic system failures are due to malfunctions of capacitors. Thus, capacitors are sometimes a reliability bottleneck. For high-voltage high-power conversion systems, dc-link capacitors are usually periodically replaced and monitored for reliable and safe operation, leading to substantial maintenance costs and electronic waste production. To enhance reliability and lifetime, high-performance capacitors, like power film capacitors, have been used as replacements for some electrolytic capacitors. As concluded, topologies for solar inverter that employ a film capacitor for power decoupling instead of aluminum electrolytic capacitors have higher mean time between failure (MTBF) and lifetime. However, the benefits of using those capacitors are to some degree compromised by their reduced volumetric efficiency and high cost. There are several prior-art approaches to lessening the dependence of the dc-link capacitance. The dc-link capacitance is reduced by allowing a larger ripple on the dc-link. Thus, there are tradeoffs between the system performance and the chosen dc-link capacitance. Some current control strategies are applied to reduce the ripple current flowing through dc-link capacitor. It relies on specific relationships in the operating frequency between the two connected converters. The performance of those controllers is sometimes affected by the accuracy of the computations and the overall time delays of the control loops. A double frequency front-end converter with multiphase switching is proposed, but the reduction of the dc-link capacitance is not significant.

OPERATION OF THE SERIES VOLTAGE COMPENSATOR

Fig. 1 shows the architecture of the grid-tie solar inverter system with a series voltage compensator connected to the dc link. The system consists of two power conversion stages. The front stage is a dc–dc boost converter. It is connected between a string of solar panels and the dc link. The output stage is a grid-tie dc–ac converter, which is connected between the dc link and the power grid.

The compensator, which is a capacitor supported full-bridge dc–ac converter without an external dc source, is connected between the two converters. The voltage compensator generates an ac voltage that counteracts the ripple voltage on the output of the boost converter. Thus, the input of the grid-tie inverter is a dc voltage equal to the average value of the voltage vdc across the dc-link capacitor Cdc. The dc-link voltage vdc and the input voltage of the voltage compensator va are sensed. The scaling factor α is the ratio between Vtric and Va,ref , where Vtric is the amplitude of the triangular carrier signal vtric in the PWM controller and Va,ref is the voltage reference for the input voltage of the voltage compensator. The difference between Va,ref and va is processed by a PI controller G(s) to give an offset voltage vos . The control signal vcon is obtained by combining α vdc with vos. The dc component of α vdc is ideally cancelled in vcon by vos as Vos = −αVdc, where Vos and Vdcare the dc component of vos and vdc, respectively. With such arrangement, it is unnecessary to use a high-pass filter to extract the ac component of vdc. At the same time, the stable dc level of va can be obtained by

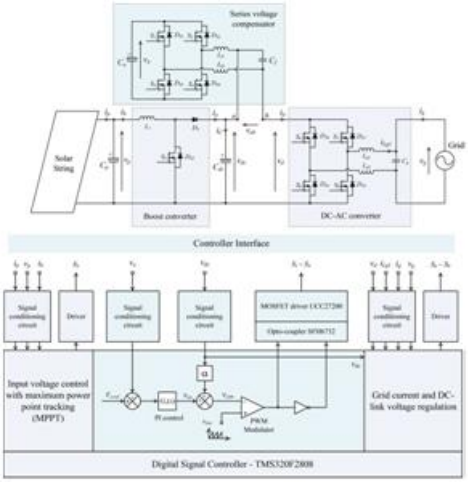

Fig. 1. Architecture of the grid-tie solar inverter with a series voltage compensator

voltage control, which ensures the compensator only handles the reactive power in the steady state. During the steady-state operation, vcon equals the conditioned ac component of αvdc.

RNI Regd No: APENG/2011/47294 ISSN No: 2320-3706(PRINT)
International Journal & Magazine of Engineering, Technology, Management and Research
YUVAENGINEERS
Transforming Young Engineers for Better Tomorrow

It is then used to compare with the triangular carrier waveform in the pulse width modulation modulator to generate the voltage vab having the same phase and amplitude with Δvdc. Without any external power supply, the power dissipation of the voltage compensator is obtained from the dc link. Practically speaking, instead of a pure ac voltage, both vab and vcon consists of not only ac component, but also small amount of the dc component. Since the input current of the grid-tie inverter consists of the dc component, some power will be absorbed by the compensator if vab consists of the dc component. Derivations of the parameters in the control.

SYSTEM CHARACTERISTICS:

The grid voltage vg and the output grid current ig can be expressed as

$$v_g(t) = V_g \sin \omega t \tag{1}$$

$$i_g(t) = I_g \sin(\omega t + \phi) \tag{2}$$

where Vg and Ig are the amplitude of vg and ig , respectively, ω = 2πf is the angular line frequency, f is the line frequency, and φ is the phase difference between vg and ig .

Based on (1) and (2), the instantaneous output power pg is

$$p_g(t) = v_g(t) i_g(t) = \frac{2P_g}{\cos \phi} \sin \omega t \sin(\omega t + \phi) \tag{3}$$

where Pg = Vg Ig 2 cos φ is the average output power. By applying the Kirchhoff's current law at the node of the dc-link capacitor Cdc, the relationship among the output current ia of the boost converter, the dc-link capacitor current iC , and input current id of the inverter can be expressed as

$$i_C(t) = i_a(t) - i_d(t). \tag{4}$$

The dominant component of Δvdc is the double of the line frequency harmonics. For the sake of simplicity in the analysis,

Δv_{dc} is expressed as

$$\Delta v_{dc}(t) = |\Delta V_{dc}| \sin(2\omega t + \theta) \tag{5}$$

where |ΔVdc| is the magnitude of Δvdc and θ is the phase angle of Δvdc.

A. Steady-State Characteristics of the Voltage Compensator:

Since the voltage compensator counteracts the ripple voltage on the dc-link capacitor only, the input voltage of the grid-tie dc–ac converter, vd , is equal to Vdc. By using (3), the input current of the dc–ac converter, id , can be expressed as

$$i_d(t) = \frac{p_g(t)}{V_{dc}} = \frac{P_g}{V_{dc} \cos \phi} [\cos \phi - \cos(2\omega t + \phi)]. \tag{6}$$

By substituting (5) and (6) into (4),

$$\gamma \cos(2\omega t + \theta - \delta) = \frac{P_g}{\lambda V_{dc} \cos \phi} \cos(2\omega t + \phi) \tag{7}$$

where $\gamma = \sqrt{\left(\frac{P_g}{V_{dc}}\right)^2 + (2\omega C_{dc} V_{dc})^2}$, $\delta = \tan^{-1}\left(\frac{P_g}{2\omega C_{dc} V_{dc}^2}\right)$, and $\lambda = \frac{|\Delta V_{dc}|}{V_{dc}}$ is the ripple factor.

Detailed proof of (7) is given in the Appendix. By equating the magnitude and phase angle of the LHS and RHS of (7), the following equations can be concluded

$$|\Delta V_{dc}| = \frac{P_g}{\gamma \cos \phi} \tag{8a}$$

$$\theta = \phi + \delta. \tag{8b}$$

By substituting (8) into (5), the ripple voltage on the dc-link capacitor is

RNI Regd No: APENG/2011/47294 ISSN No: 2320-3706(PRINT)
International Journal & Magazine of Engineering, Technology, Management and Research
YUVAENGINEERS
Transforming Young Engineers for Better Tomorrow

$$\Delta v_{\mathrm{dc}}(t) = \frac{P_g}{\gamma \cos\phi} \sin(2\omega t + \phi + \delta)$$
$$= \lambda V_{\mathrm{dc}} \sin(2\omega t + \phi + \delta). \quad (9)$$

According to (9), the relationship among the dc-link capacitance Cdc, output phase angle φ, and the ripple factor λ is

$$C_{\mathrm{dc}} = \frac{S_g}{2\omega V_{\mathrm{dc}}^2} \sqrt{\frac{1}{\lambda^2} - \cos^2\phi} \quad (10)$$

The first term αPg sin(2ωt+φ+δ) γVt r ic cos φ va (t) represents the ripple voltage compensation on the dc-link capacitor. The second term αVd c+vo s (t) Vt r ic va (t) represents the dc component, related to the power balance described in (13). Thus, asymmetrical PWM switching occurs. Fig. 2(a) and (b) present the operating modes of the compensator using a full bridge. When S2 and S3 are on, the capacitor Ca is charged by the load current id . Conversely, when S1 and S4 are on, the capacitor Ca is discharged by id. Fig. 2(c) shows the waveforms of the dc-link capacitor voltage vdc, modulating signal vm, triangular carrier signal vtric , and the voltage across Ca , va . The dc component on vab is very small. It is observed to be 2.1 V, about 0.5% of the average dc-link voltage of 400 V in the 2-kW inverter system, which will be described in Section V. Thus, such dc component is neglected in the following discussion.

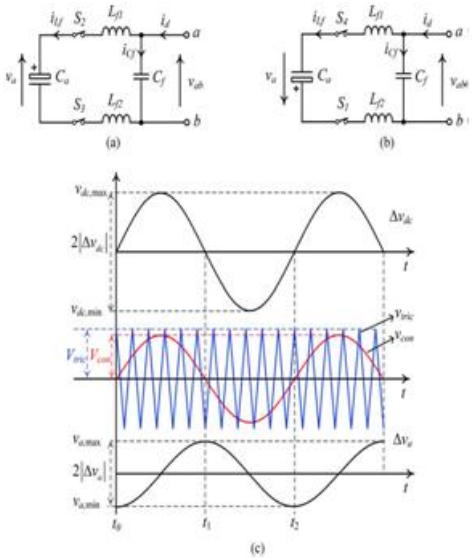

Fig. 2. Ripple voltage on the input capacitor Ca in the compensator. (a) Operation when S2 and S3 are on. (b) Operation when S1 and S4 are on. (c) SPWM and the ripple voltage generated across Ca

During the time interval between the time instants t0 and t1 in Fig. 2(c), Ca is charged by the load current. By using (6) and (9).

DESIGN GUIDELINES:

By using (10) and (16), the relationships between Cdc – λ and Ca − λ are depicted in Fig. 7. The parameters used in the analysis are given in Table I. The value of λ increases as the value of Cdc reduces. Thus, a film capacitor bank can be used for Cdc. However, the required value of Ca increases as λ increases and its voltage ripple (i.e., |ΔVa |/Va) reduces. As Va _ Vdc, low-voltage electrolytic capacitors of long lifetime can be used for Ca , and switching devices of low voltage rating can be used for S1 ∼ S4 . Apart from the static characteristics, the value of Ca is also determined by studying the dynamic response of the compensator.

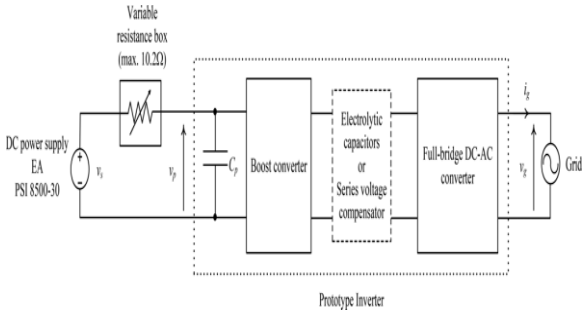

Fig.. Test bed for the prototype 2-kW, 220-V, 50-Hz solar inverter

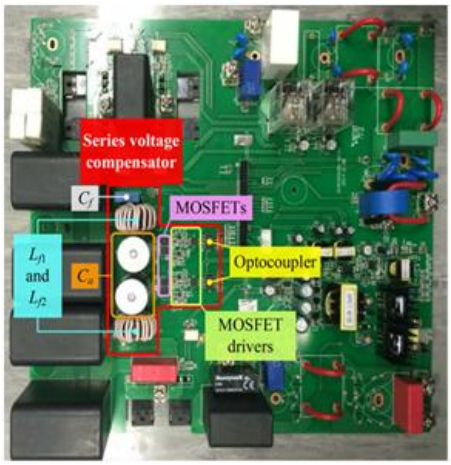

RNI Regd No: APENG/2011/47294 ISSN No: 2320-3706(PRINT)
International Journal & Magazine of Engineering, Technology, Management and Research
YUVAENGINEERS
Transforming Young Engineers for Better Tomorrow

Reduces as Ca increases. Thus, the design is based on considering the required low-frequency response of the voltage compensator. Take a 2-kW solar inverter system that will be discussed in Section V as an example. If the designed ripple voltage on Cdc is 10%, the required value for Cdc is 220 μF. Two parallel connected 110 μF/450 V power film capacitors are used. If the allowed ripple voltage on Ca is 5%, the required value for Ca is 2546 μF. If the allowed ripple voltage on Ca is 10%, the required value for Ca is 1273 μF. Hence, two 1000 uF/63 V long lifetime electrolytic capacitors [27] can be used. Taking Ca= 2000 μF for depicting bode diagram of ΔVab (s)/ΔVdc(s) in Fig. 8, it can be seen that, the magnitude is nearly unity and the phase difference is almost zero in the frequency 100 Hz of ripple voltage. Then, the two parallel connected 1000 μF/63 V long lifetime electrolytic capacitors will meet the design requirement for Ca. The effects of the variation of the capacitance on both the static and dynamic characteristics of the system are studied.

Fig. 7 depicts how the ripple voltage on the dc link (i.e., ΔVdc/Vdc) and on the capacitor Ca (i.e., va) in the compensator are varied with the reduction of the values of the dc-link capacitor Cdc and of the capacitor Ca in the compensator. For example, when Cdc is reduced from 275 to 220 μF, the per-unit ripple voltage on Cdc (or dc link) is increased from 0.08 to 0.1. If the value of Ca is kept at 2037 μF with Cdc changing from 275 to 220 μF (20% reduction), the ripple voltage on Ca will change from 5% to 6.2%. If Cdc is reduced from 275 to 220 μF and Ca is reduced from 2037 to 1630 μF (20% reduction), the ripple voltage on Ca is changed from 5% to 7.8%. Fig. 8 shows the frequency response of the variation of the compensator output voltage to the variation of the dc-link voltage. (38) reveals that the frequency response is dependent on the value of Ca and is less dependent on Cdc. It is because the compensator mainly responds to the variation of the dc-link voltage and its dynamic response is affected by the value of Ca .

As shown in Fig. 8, the corner frequency will shift to a higher frequency when Ca is reduced. For example, if Ca is changed from 2000 μF (which is the chosen value in the design) to 500 μF (reduction by 75%), the corner frequency will move from 10 to 40 Hz. The operation is still acceptable as the dominant frequency component handled by the compensator is 100 Hz.

CONCLUSION:

This paper extends the study of the concept proposed, in which a series voltage compensator is used to reduce the dc-link capacitance. Such concept is applied to a grid-tie solar inverter. The modeling and design of the series voltage compensator has been presented. Compared this paper has the following distinctive discussions:

1) The steady-state power managed by the series voltage compensator is relatively constant in the ac–dc–dc system discussed, while the solar inverter has to process time-varying ac power. Thus, interactions among the front-stage boost converter, compensator, and output dc–ac converter, have been discussed.

2)The static characteristics of the series voltage compensator only, while this paper gives both static and dynamic characteristics of the whole system.

3) The external characteristics of the whole system have been given.

4) A detailed comparison on the implementation costs of the electrolytic capacitors and series voltage compensator has been given.

A 2 kW, 220-V, 50-Hz prototype inverter has been built to compare the results with the electrolytic capacitors and with the compensator, respectively. The experimental results show that, with the compensator, a 90% reduction of dc-link capacitance and more than eight times extension of estimated lifetime can be achieved. The frequency response of the entire system is also verified by experiment.

RNI Regd No: APENG/2011/47294 ISSN No: 2320-3706(PRINT)
International Journal & Magazine of Engineering, Technology, Management and Research
YUVAENGINEERS
Transforming Young Engineers for Better Tomorrow

The implementation cost of the compensator is comparable to that of electrolytic capacitors for 400-V applications. For 800-V applications, the implementation cost of the compensator is lower than that of the electrolytic capacitors. The main reason is that multiple series-connected electrolytic capacitors are needed for high-voltage applications, while film capacitors of high-voltage rating are available.

REFERENCES:

[1]A. Braham, A. Lahyani, P. Venet, and N. Rejeb, "Recent developments in fault detection and power loss estimation of electrolytic capacitors," IEEE Trans. Power Electron, vol. 25, no. 1, pp. 33–43, Jan. 2010.

[2]N.Blattau andC.Hillman, "Has the electronics industrymissed the boat on Pb-free?–failures in ceramic capacitors with Pb-free solder interconnects," in Proc. 5th Int. Lead Free Conf. Electron. Components Assemblies, San Jose, CA, USA, Mar. 18–19, 2004.

[3]G. Terzulli, Film Technology to Replace Electrolytic Technology in Wind Power Applications, AVX Technical Note, 2010.

[4]Film Capacitors for Industrial Applications, EPCOS Application Note, EPCOS AG, Munich, Germany, 2007.

[5]S. Harb and R. S. Balog, "Reliability of candidate photovoltaic module integrated- inverter (PV-MII) topologies—a usage model approach," IEEE Trans. Power Electron., vol. 28, no. 6, pp. 3019–3026, Jun. 2013.

[6]P. Pelletier, J. M. Guichon, J. L. Schanen, and D. Frey, "Optimization of a DC capacitor tank," IEEE Trans. Ind. Appl., vol. 45, no. 2, pp. 880–886, Mar./Apr. 2009.

[7]D. Lamar, J. Sebastian, M. Arias, and A. Fernandez, "On the limit of the output capacitor reduction in power-factor correctors by distorting the line input current," IEEE Trans. Power Electron., vol. 27, no. 3, pp. 1168–1176, Mar. 2012.

[8]I. S. Freitas, C. B. Jacobina, and E. C. Santos Jr., "Single-phase to singlephase full-bridge converter operating with reduced AC power in the DClink capacitor," IEEE Trans. Power Electron., vol. 25, no. 2, pp. 272–279, Feb. 2010.